Median nerve stimulation induces analgesia via orexin-initiated endocannabinoid disinhibition in the periaqueductal gray

Yi-Hung Chen (陳易宏)[a,b,c], Hsin-Jung Lee (李欣蓉)[d,1], Ming Tatt Lee (李鳴達)[d,e,f,1], Ya-Ting Wu (吳雅婷)[a], Yen-Hsien Lee (李彥賢)[g], Ling-Ling Hwang (黃玲玲)[g,h], Ming-Shiu Hung (洪明秀)[i], Andreas Zimmer[j], Ken Mackie[k,l], and Lih-Chu Chiou (邱麗珠)[a,d,e,2]

[a]Graduate Institute of Acupuncture Science, China Medical University, Taichung, Taiwan 40402; [b]Chinese Medicine Research Center, China Medical University, Taichung, Taiwan 40402; [c]Department of Photonics and Communication Engineering, Asia University, Taichung, Taiwan 41354; [d]Department of Pharmacology, College of Medicine, National Taiwan University, Taipei, Taiwan 10051; [e]Graduate Institute of Brain and Mind Sciences, College of Medicine, National Taiwan University, Taipei, Taiwan 10051; [f]Faculty of Pharmaceutical Sciences, UCSI University, 56000 Kuala Lumpur, Malaysia; [g]Graduate Institute of Biomedical Sciences, College of Medicine, Taipei Medical University, Taipei, Taiwan 110; [h]Department of Physiology, College of Medicine, Taipei Medical University, Taipei, Taiwan 110; [i]Institute of Biotechnology and Pharmaceutical Research, National Health Research Institutes, Zhunan, Miaoli County, Taiwan 35053; [j]Institute for Molecular Psychiatry, University of Bonn, 53113 Bonn, Germany; [k]Gill Center for Biomolecular Research, Indiana University, Bloomington, IN 47405; and [l]Department of Psychological and Brain Sciences, Indiana University, Bloomington, IN 47405

Adequate pain management remains an unmet medical need. We previously revealed an opioid-independent analgesic mechanism mediated by orexin 1 receptor (OX1R)-initiated 2-arachidonoylglycerol (2-AG) signaling in the ventrolateral periaqueductal gray (vlPAG). Here, we found that low-frequency median nerve stimulation (MNS) through acupuncture needles at the PC6 (Neiguan) acupoint (MNS-PC6) induced an antinociceptive effect that engaged this mechanism. In mice, MNS-PC6 reduced acute thermal nociceptive responses and neuropathy-induced mechanical allodynia, increased the number of c-Fos–immunoreactive hypothalamic orexin neurons, and led to higher orexin A and lower GABA levels in the vlPAG. Such responses were not seen in mice with PC6 needle insertion only or electrical stimulation of the lateral deltoid, a nonmedian nerve-innervated location. Directly stimulating the surgically exposed median nerve also increased vlPAG orexin A levels. MNS-PC6–induced antinociception (MNS-PC6-IA) was prevented by proximal block of the median nerve with lidocaine as well as by systemic or intravlPAG injection of an antagonist of OX1Rs or cannabinoid 1 receptors (CB1Rs) but not by opioid receptor antagonists. Systemic blockade of OX1Rs or CB1Rs also restored vlPAG GABA levels after MNS-PC6. A cannabinoid (2-AG)-dependent mechanism was also implicated by the observations that MNS-PC6-IA was prevented by intra-vlPAG inhibition of 2-AG synthesis and was attenuated in $Cnr1^{-/-}$ mice. These findings suggest that PC6-targeting low-frequency MNS activates hypothalamic orexin neurons, releasing orexins to induce analgesia through a CB1R-dependent cascade mediated by OX1R-initiated 2-AG retrograde disinhibition in the vlPAG. The opioid-independent characteristic of MNS-PC6–induced analgesia may provide a strategy for pain management in opioid-tolerant patients.

median nerve stimulation | orexin | endocannabinoid | periaqueductal gray | analgesia

Recently, several US federal agencies, led by the NIH, jointly funded a total of US $81 million over 6 y for research projects on nondrug approaches for pain management and related conditions. Nondrug treatments are being recognized as a viable approach to address the urgency of the public health crisis of pain as well as the opioid epidemic (1). Peripheral neuromodulation has been used for relieving intractable chronic pain since the 1960s (2) based on the gate theory proposed by Melzack and Wall (3). More recently, it has also been used to manage chronic pain conditions such as migraine, neuropathic pain, and lower back pain (4, 5). After several decades of clinical practice, the safety and efficacy of peripheral neuromodulation are gradually being appreciated. The US Food and Drug Administration (FDA) recently approved a peripheral neuromodulation device

designed to treat chronic refractory pain (6, 7). However, the analgesic mechanisms of peripheral neuromodulation remain unclear. In the 1960s, the gate control theory was considered an adequate explanation (3). However, it is now known that more complex supraspinal mechanisms are involved in pain control (8), particularly that elicited by peripheral electrical stimulation (9). Both peripheral and central mechanisms (10–12), especially those involving opioid, dopamine, noradrenaline, and serotonin systems (13–15), have been proposed to underlie the efficacy of peripheral neuromodulation. In this study, we aim to discern central mechanism(s) of peripheral neuromodulation elicited via median nerve stimulation (MNS).

MNS has been known to effectively relieve chronic pain for more than 50 y (2, 16). In the pioneering report by Wall and Sweet (2), MNS by an implanted stimulator led to temporary pain relief in a patient with intractable chronic pain caused by a

Significance

Pain remains an unmet medical need due to the ineffectiveness or significant side effects of current pain therapies. Peripheral neurostimulation has been used to relieve pain for decades, but its mechanism(s) remain unsettled. Here, we established an animal model of median nerve stimulation by electrically stimulating the PC6 (Neiguan) acupoint of mice (MNS-PC6). We found MNS-PC6 can release an endogenous neuropeptide (orexin) from the hypothalamus to inhibit pain responses in mice through an endocannabinoid (an endogenous lipid functioning like chemicals from cannabis) that reduces the inhibitory (GABAergic) control in a midbrain pain-control region (the periaqueductal gray). Importantly, MNS-PC6–induced pain relief is endogenous opioid independent. Thus, MNS-PC6 may provide an alternative strategy for pain management in opioid-tolerant patients.

fractured elbow. Several reports have subsequently demonstrated significant pain relief after MNS with surgically implanted electrodes in patients with intractable peripheral neuropathic pain or complex regional pain syndrome (17–24). Notably, electrical stimulation of the median nerve remained effective after 18–24 y of follow-up in two patients (19) and for 3–16 y of follow-up in four of six patients and was accompanied by discontinuation of analgesic medicines (23). MNS also suppressed dysmenorrhea, and this effect was opioid independent (25) and without tolerance (26). Interestingly, MNS was effective in alleviating chronic pain not only locally at median nerve-innervated regions (18, 20, 21) but also at painful regions far away from the median nerve (25, 27). The latter studies suggest that MNS-induced analgesia is not limited to a local effect. A study in primates showed that spinothalamic tract activation by a painful stimulation at the sural nerve can be inhibited by activating the ipsilateral or contralateral median nerve (28), suggesting that MNS blocks pain signals via a central mechanism(s). Among the brain regions involved in pain modulation, the periaqueductal gray (PAG), which is an important midbrain region for initiating descending pain inhibition (29–31), is a possible central site of action for MNS. Importantly, activation of the PAG inhibits spinothalamic tract neuronal activity in primates (32) and rats (33) and can induce analgesia via a nonopioid mechanism (34) distinct from the well-known opioid mechanism (35). We therefore hypothesized that peripheral MNS activates the PAG, leading to opioid-independent analgesia.

Previously, we demonstrated a nonopioid analgesic mechanism mediated by endocannabinoids that can be induced by orexin A in the ventrolateral PAG (vlPAG) (36), an important site for antinociceptive actions of cannabinoids (37). Orexin A and orexin B, also named "hypocretin 1" and "hypocretin 2," are a pair of neuropeptides derived from prepro-hypocretin and are expressed in neurons limited to the perifonical area (PFA) and lateral hypothalamus (LH) (38, 39). These neurons project widely throughout the central nervous system, including the PAG (40, 41), a brain region activated by intracerebroventricular orexin (42) and that also has abundant orexin receptors (43). Our study demonstrated that orexin A activates postsynaptic orexin 1 receptors (OX1Rs) in the vlPAG, resulting in synthesis of 2-arachidonoylglycerol (2-AG), an endocannabinoid, via a phospholipase C (PLC)–diacylglycerol lipase (DAGL) enzymatic pathway. 2-AG then produces retrograde inhibition of GABA release (disinhibition) by activating presynaptic cannabinoid 1 receptors (CB1Rs) in the vlPAG. Inhibition of the abundant PAG GABAergic interneurons (44) activates excitatory PAG neurons projecting to the rostroventral medulla (RVM) that in turn send inhibitory projections to the spinal cord dorsal horn, culminating in the activation of the descending pain inhibitory pathway that is constituted by the PAG–RVM–spinal dorsal horn circuit (36) and ultimately leading to analgesia. Using retrograde tracing, electron microscopy, and in vivo electrophysiological approaches, Cristino et al. (45, 46) showed that RVM-projecting vlPAG neurons were DAGL/OX1R-immunoreactive and that these neurons receive CB1R-containing inhibitory inputs and orexinergic inputs, providing anatomical evidence supporting the involvement of OX1R–2-AG–CB1R signaling in descending pain inhibition.

Interestingly, when investigating the cardiovascular depressant effect of electroacupuncture (EA) in rats, the Longhust group (47, 48) demonstrated that electrical stimulation at acupoints PC5 (Jianshi) and PC6 (Neiguan) induced a CB1R-mediated inhibition of GABA release in the vlPAG. This suggests that EA at these acupoints induces an endocannabinoid-dependent inhibition of GABA release in the vlPAG. The PC5 and PC6 acupoints are known to overlie the median nerve in humans (49). Moreover, EA at the PC6 acupoint, i.e., EA-PC6, has been reported to be relevant to MNS, as both procedures electrically stimulate MN-innervated dermatomes (50–52). We therefore hypothesized that

electrical stimulation of the median nerve activates hypothalamic orexin neurons, releasing orexin A into the vlPAG and triggering the disinhibition mechanism mediated by the OX1R–PLC–DAGL–2-AG–CB1R cascade in the vlPAG, leading to analgesia.

Results

MNS at PC6 Increased the Withdrawal Latency in the Mouse Hot-Plate Test.
Anesthetized mice were subjected to 2-Hz electrical MNS targeted at PC6 (MNS-PC6) (*SI Appendix*, Fig. S1) for 20 min, were allowed to recover from anesthesia, and then were subjected to the hot-plate test (Fig. 1). This MNS-PC6 group of mice displayed hot-plate withdrawal latencies that were significantly longer than their baseline withdrawal latencies (Fig. 2A). The effect of MNS-PC6–induced analgesia (MNS-PC6-IA) was time-dependent (*SI Appendix*, Table S1), being maximal at 10 min after MNS, followed by gradual decreases, lasting for about 60 min (Fig. 2A). The mice in the control group that received only anesthesia, in the sham group that received acupuncture needle insertion but no electrical stimulation, and in the non-MNS group that received electrical stimulation through acupuncture needles inserted at the nonmedian nerve-innervated lateral deltoid muscles (*Materials and Methods*) did not show a significant change in the hot-plate withdrawal latency (Fig. 2A). Thus, there was a significant antinociceptive effect, calculated by the area under the curve (AUC) (latency × min) (*Materials and Methods*), in the MNS-PC6 group compared with the control groups (Fig. 2B). However, the AUCs among the control (69.08 ± 18.53, $n = 6$), sham (81.19 ± 56.16, $n = 6$), and non-MNS (44.53 ± 27.85, $n = 5$) groups were not significantly different ($P = 0.625$, Kruskal–Wallis test). These results suggest that a 20-min low-frequency electrical stimulation at PC6, but not at a nonmedian nerve-innervated location, induces a significant antinociceptive effect lasting about 1 h in mice, while anesthesia, needle insertion at PC6 alone, or electrical stimulation at a nonmedian nerve-innervated location did not have this effect.

MNS-PC6-IA Was Reduced by Systemic Pretreatment with an OX1R or CB1R Antagonist.
To validate our hypothesis that MNS-PC6-IA is mediated by OX1R-mediated endocannabinoid signaling, we examined whether MNS-PC6-IA was blocked by an OX1R (SB 334867) or CB1R (AM251) antagonist. Indeed, MNS-PC6-IA was markedly reduced by i.p. pretreatment with SB 334867
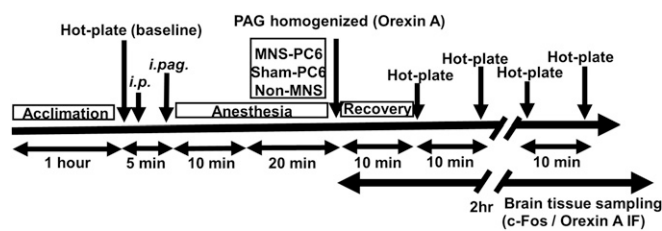

Fig. 1. Timeline for procedures (drug administration, anesthesia, blood and brain tissue sampling) and hot-plate tests before and after MNS-PC6. After 1 h of acclimation, mice were anesthetized for 10 min and given MNS-PC6 for 20 min under 2% isofluorane. The hot-plate test was conducted before any procedure (baseline), 10 min after MNS-PC6 termination, and every 10 min thereafter for 60 min. MNS-PC6 was performed by electrical stimulation (2 Hz, 2 mA, 0.15 ms) at the PC6 (Neiguan) acupoint, which was determined relative to its anatomical location described in the WHO guidelines for human acupoints (58). The sham group received acupoint needle insertion only. The control group received anesthesia only. The non-MNS group received electrical stimulation in the lateral deltoid muscle, an anatomical location not innervated by the median nerve. The locations of PC6 and non-MNS in a mouse, described in *Materials and Methods*, are depicted in *SI Appendix*, Fig. S1. Drugs were given by i.p. injection 15 min before or by i.pag. microinjection 10 min before MNS-PC6. vlPAG orexin A levels were measured immediately after MNS-PC6 termination. Orexin A/c-Fos immunofluorescence in the LH was measured 2 h after MNS-PC6 termination.
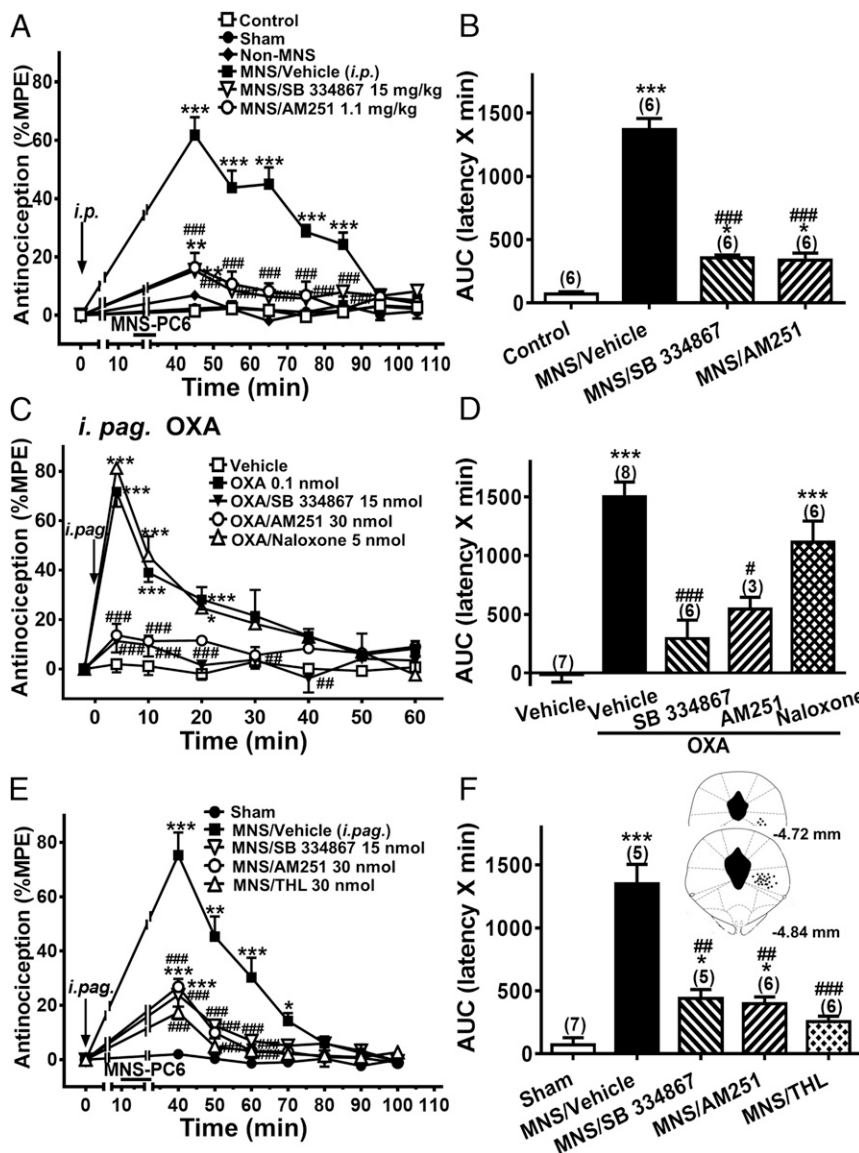
Chen et al.

NEUROSCIENCE

www.manaraa.com

Fig. 2. Effects of MNS-PC6 or i.pag. orexin on the mouse hot-plate test and their interactions with OX1R, CB1R, opioid receptor antagonists, and a DAGL inhibitor. Antinociceptive effects of MNS-PC6 (*A*, *B*, *E*, and *F*) or i.pag. orexin A (*C* and *D*) with i.p. (*A* and *B*) or i.pag. (*E* and *F*) pretreatment or i.pag. coadministration (*C* and *D*) with an OX1R antagonist (SB 334867), CB1R antagonist (AM251), DAGL inhibitor (THL), or vehicle. (*A*, *C*, and *E*) Time courses of antinociceptive effects are expressed as the percentage of MPE (%MPE). Arrows indicate drug administration; horizontal bars indicate MNS-PC6. *$P <$ 0.05, **$P <$ 0.01, ***$P <$ 0.001 vs. the control (*A*), vehicle alone (*C*), or sham (*E*) group; #$P <$ 0.05, ##$P <$ 0.01, ###$P <$ 0.001 vs. the MNS/vehicle (*A* and *E*) or orexin A/vehicle (*C*) group (two-way ANOVA with repeated measures over time/Bonferroni's post hoc test). (*B*, *D*, and *F*) Antinociceptive effects are expressed as the AUC. Comparison groups are the same as in *A*, *C*, and *E*, except *,#$P <$ 0.05/n, **,##$P <$ 0.01/n, ***,###$P <$ 0.001/n (n was 6, 8 and 10 in *B*, *D*, and *F*, respectively; Kruskal–Wallis test/Mann–Whitney *U* post hoc test with the Bonferroni correction with n independent hypotheses; see also *SI Appendix*, Table S2). (*Inset* in *F*) Microinjection sites taken from all mice with successful injections in the vlPAG depicted in two PAG sections at bregma −4.72 and −4.84 mm, respectively. Injection sites were confirmed by trypan blue injected through the microinjection cannula after the hot-plate test. The numbers in parentheses over the bars in *B*, *D*, and *F* indicate the number of animals used in each group.

(15 mg/kg) or AM251 (1.1 mg/kg) 15 min before MNS-PC6 (Fig. 2 *A* and *B*). The antagonist effects were persistent (Fig. 2*A* and *SI Appendix*, Table S1). Neither antagonist affected the hot-plate nociceptive response per se (*SI Appendix*, Fig. S3*A*). As indicated by the AUC, the reduction of MNS-PC6-IA induced by SB 334867 (74.1 ± 1.8%, $n = 6$) was comparable to that induced by AM251 (75.4 ± 4.1%, $n = 6$; $P = 0.5887$, Mann–Whitney *U* test) (Fig. 2 *A* and *B*). This suggests that MNS-PC6-IA requires activation of both OX1Rs and CB1Rs by endogenous orexins and endocannabinoids, respectively.

IntravlPAG Microinjection of Orexin A Induced an Antinociceptive Effect Mediated by OX1Rs and CB1Rs but Not by Opioid Receptors. Previously, we have shown that exogenous orexin induced a significant antinociceptive effect in the hot-plate test that was abolished by intra-vlPAG microinjection (i.pag.) of SB 334867 and AM251 in the hot-plate test in rats (36) and mice (53). Here, we reproduced the antinociceptive effect of i.pag. orexin A in the mouse hot-plate test (Fig. 2 *C* and *D* and *SI Appendix*, Table S1). At 0.1 nmol, i.pag. orexin A produced a significant antinociceptive effect compared with the vehicle group (Fig. 2*D*). This antinociceptive effect is comparable to that of MNS-PC6-IA, as indicated by the AUC

(latency × min) for orexin A (1,502 ± 67, $n = 8$) (Fig. 2*D*) vs. MNS-PC6-IA (1,368 ± 88, $n = 6$; $P = 0.7466$, Mann–Whitney *U* test) (Fig. 2*B*). Importantly, the antinociceptive effect of orexin A was substantially reduced by i.pag. pretreatment with SB 334867 (15 nmol) or AM251 (30 nmol) but not by naloxone (5 nmol) (Fig. 2 *C* and *D*). This dose of naloxone effectively antagonized i.pag. morphine (13 nmol)-induced antinociception (53). These results suggest that MNS-PC6 induces an antinociceptive effect comparable to that produced by exogenous orexin, which is mediated via an opioid-independent mechanism involving OX1Rs and CB1Rs in the vlPAG.

MNS-PC6-IA Was Reduced by IntravlPAG Pretreatment with an OX1R or CB1R Antagonist or a DAGL Inhibitor. To further examine whether MNS-PC6-IA is mediated via the OX1Rs and CB1Rs in the PAG, we applied OX1R and CB1R antagonists by i.pag. microinjection. IntravlPAG pretreatment with SB 334867 (15 nmol) or AM251 (30 nmol), the same doses that antagonized i.pag. orexin A-induced antinociception, markedly reduced MNS-PC6-IA in mice (Fig. 2 *E* and *F*). Moreover, MNS-PC6-IA was also significantly reduced by i.pag. pretreatment with tetrahydrolipstatin (THL) (30 nmol), which inhibits the 2-AG–synthesizing enzyme DAGL (54). All three antagonists had no effect when

www.manaraa.com

administered alone (*SI Appendix*, Fig. S2*B*). Interestingly, the reductions of MNS-PC6-IA induced by i.pag. SB 334867 (67.5 ± 5.3%, n = 5), AM251 (70.5 ± 4.0%, n = 6), and THL (80.9 ± 3.1%, n = 6) were comparable (P = 0.086, Kruskal–Wallis test) (Fig. 2*F*) and are also similar to the reductions induced by i.p. injection of either antagonist (P = 0.1613, Kruskal–Wallis test) (Fig. 2*B*). These results suggest that MNS-PC6-IA is mediated by a mechanism involving OX1Rs, CB1Rs, and 2-AG in the vlPAG, which is likely to be the OX1R–PLC–DAGL–2AG–CB1R cascade in the vlPAG we reported previously (36).

MNS-PC6 Increased the Number of Activated Hypothalamic Orexin Neurons. We next examined whether MNS-PC6 activates hypothalamic orexin neurons by measuring the number of orexin neurons in the LH and PFA expressing c-Fos protein, a widely used marker of neuronal activation (55). Double immunofluorescent labeling of c-Fos protein and orexin A in the LH and PFA was conducted in hypothalamic tissues harvested 2 h after MNS termination (Fig. 1).

The number of orexin A-immunoreactive neurons in both the LH and PFA was similar among the MNS-PC6, non-MNS, and control groups (Fig. 3 *A* and *B*). However, the number of neurons that were immunopositive for both orexin A and c-Fos was significantly higher in the MNS-PC6 group than in the non-MNS and control groups (Fig. 3 *A* and *C*). This resulted in a higher percentage of orexin neurons expressing c-Fos in the MNS-PC6 group (Fig. 3*C*). Neither the total number of orexin neurons nor the number of c-Fos–containing neurons differed between the non-MNS and control groups (Fig. 3). The number of c-Fos–containing neurons in both LH and PFA regions was also higher in the MNS-PC6 group, but not in the non-MNS group, compared with the control group (Fig. 3*D*).

MNS-PC6 Increased Orexin A Levels and Decreased GABA Levels in the vlPAG. Next, we measured orexin A levels in vlPAG homogenates from mice after termination of MNS by enzyme immunoassay (EIA) (Fig. 1). As predicted, the MNS-PC6 group had higher orexin A levels in the vlPAG than the non-MNS or control groups; the latter two groups had similar levels (Fig. 4*A*).

To further examine whether MNS-PC6 induces disinhibition in the vlPAG, we measured GABA levels in microdialysates collected from the vlPAG of mice. Mean baseline GABA levels in the vlPAG of anesthetized mice before any treatment did not differ significantly among the control (31 ± 3.6 nM), MNS-PC6 (35 ± 3.8 nM), and non-MNS (31 ± 3.7 nM) groups. These vlPAG GABA levels in mice are similar to those found in rats (37–38 nM) (47). As shown in Fig. 4*B*, in the MNS-PC6 group, the average GABA level in the vlPAG microdialysate was significantly decreased after MNS-PC6 compared with the level before MNS-PC6, but GABA levels were not significantly altered in the non-MNS or control groups. The MNS-PC6–induced attenuation of GABA levels in the vlPAG was prevented by i.p. pretreatment with SB 334867 or AM251 (Fig. 4*C*). Neither of these antagonists affected GABA levels in the non-MNS or control groups (Fig. 4*D*).

These results suggest that MNS-PC6 activates LH orexin neurons to release orexin A in the vlPAG, inducing analgesia via an opioid-independent mechanism by inhibiting GABA release (disinhibition) in the vlPAG via an OX1R–2-AG–CB1R sequential cascade (36).

Effects of MNS-PC6 on the Hot-Plate Nociceptive Response in *Cnr1*⁻/⁻ Mice. To confirm the contribution of the OX1R–2-AG–CB1R cascade in MNS-PC6-IA, we studied MNS-PC6-IA in *Cnr1*⁻/⁻ mice, which lack CB1Rs globally (56), and in WT mice. MNS-PC6 induced a much weaker antinociceptive effect in *Cnr1*⁻/⁻ mice than in WT mice (Fig. 5). This supports the notion that MNS-PC6-IA is primarily elicited by a CB1R-mediated mechanism. However, the baseline hot-plate withdrawal latency was significantly longer in *Cnr1*⁻/⁻ mice than in WT mice (Fig. 5*A*), as
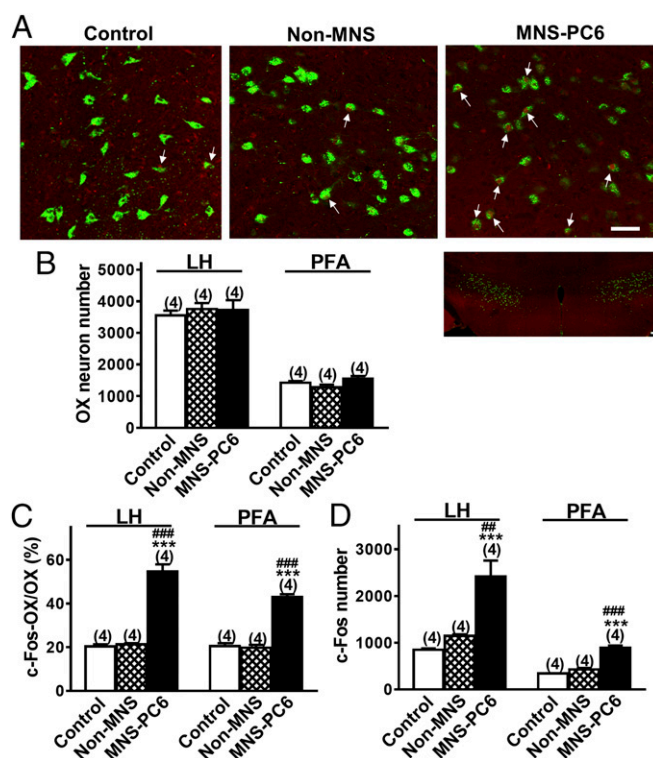
Fig. 3. MNS-PC6 increased the number of c-Fos–expressing orexin neurons in the LH and PFA as well as orexin A levels in the vlPAG. (*A*) Merged confocal micrographs of mouse LH sections double-immunofluorescently labeled with anti-orexin A antibody (green) and anti–c-Fos antibody (red) in the control (*Left*), non-MNS (*Center*), and MNS-PC6 (*Right*) groups. Hypothalamic cells labeled with green in the cytoplasm and red in the nucleus area are indicative of orexin A and c-Fos coexpression (arrows). (Scale bar: 50 μm.) (*Lower Right*) A lower-magnification confocal micrograph of a mouse hypothalamus section taken from the MNS-PC6 control group. The central hole is the third ventricle. (Scale bar: 100 μm.) (*B–D*) The total number of orexin A-immunoreactive neurons (OX) (*B*), the percentage of c-Fos–expressing orexin neurons (Fos-OXA) among total orexin neurons (OX) (*C*), and the number of c-Fos–expressing neurons (c-Fos) (*D*) in one side of the LH and PFA in the control, non-MNS, and MNS-PC6 groups. Double immunofluorescent staining was conducted in LH and PFA tissue sections harvested 2 h after MNS-PC6 termination. Fos-OXA, OXA, and c-Fos neurons were counted using the Stereo Investigator (MBF Bioscience). ##P < 0.01; ***P < 0.001 vs. control; ###P < 0.001 vs. non-MNS (one-way ANOVA/Tukey's post hoc test). The numbers in parentheses over the bars in *B–D* indicate the number of mice used in each group.

previously noted (56). It remains to be elucidated whether the elevated nociceptive threshold in *Cnr1*⁻/⁻ mice renders them less susceptible to any analgesic compounds, including opioids or nonsteroidal antiinflammatory drugs, whose mechanism of action is unrelated to endocannabinoids.

Direct MNS also Increased Orexin A Levels in the vlPAG. To confirm that the orexin-mediated antinociceptive effect induced by the MNS-PC6 procedure is indeed produced by MNS, we examined whether direct median nerve stimulation (DMNS) also activates the orexin system. In the DMNS group, we directly stimulated the surgically exposed median nerve with the same stimulation parameters (2 Hz and 20 ms for 20 min) applied for MNS-PC6 but at a lower current (1 mA instead of 2 mA). In the sham-treated group of mice (sham-DMNS), the stimulating electrode was placed beside the median nerve, but the nerve was not electrically stimulated (Fig. 6*A*). Orexin A levels in the vlPAG of mice receiving DMNS for 20 min were significantly higher than in the control group that received anesthesia only and in the sham-DMNS group (Fig. 6*B*), and this level (2.807 ± 0.2043 pg/μg) (Fig. 6*B*) was comparable
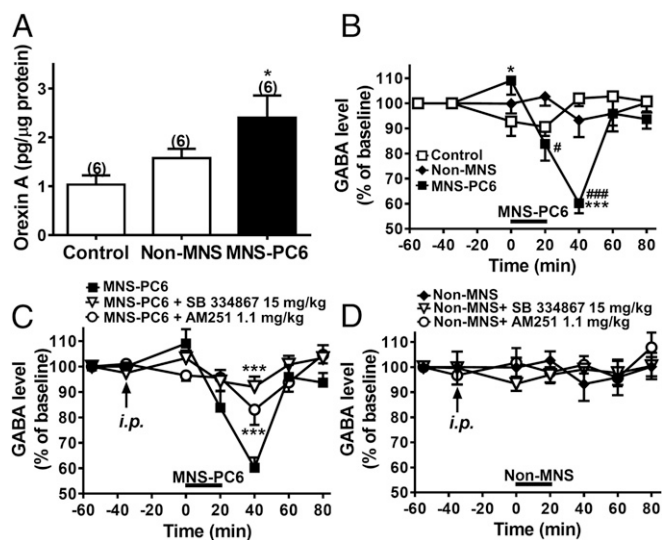
www.manaraa.com

Fig. 4. MNS-PC6 increased orexin A levels and decreased GABA levels in the vlPAG in a manner prevented by systemic SB 334867 and AM251. (*A*) Orexin A levels in vlPAG homogenates prepared from mice in the MNS-PC6, non-MNS, and control groups. Immediately after MNS-PC6 termination, the vlPAG in each mouse was micropunched bilaterally and homogenized. Orexin A levels in the vlPAG homogenate were measured with EIA. *$P <$ 0.05 vs. control (one-way ANOVA/Tukey's post hoc test). (*B*) GABA levels in vlPAG microdialysates of anesthetized mice in the MNS-PC6, non-MNS, and control groups. GABA levels in the vlPAG microdialysate sampled from 75–55, 55–35, and 20–0 min before, during, and every 20 min after MNS-PC6 or non-MNS treatment for 1 h in each mouse were measured by HPLC and expressed as the percentage of the baseline level in each mouse, which was the mean GABA concentration before treatment. Results from control mice receiving only anesthesia were also compared. *$P <$ 0.05, ***$P <$ 0.001 vs. control and #$P <$ 0.05, ###$P <$ 0.001 vs. non-MNS (two-way ANOVA with repeated measures over time/Bonferroni's post hoc test), $n = 6$. (*C* and *D*) GABA levels in vlPAG microdialysates of mice before and after MNS-PC6 (*C*) or non-MNS (*D*) with or without pretreatment with SB 334867 or AM251. The antagonist was given by i.p. injection (arrows) at 35 min before MNS-PC6 or non-MNS (horizontal bars). In *C*, ***$P <$ 0.001 vs. MNS-PC6 (two-way ANOVA with repeated measures over time/Bonferroni's post hoc test), $n = 6$. The numbers in parentheses over the bars in *A* indicate the number of mice used in each group.

to that in the MNS-PC6 group (2.404 ± 0.4569 pg/μg; $P = 0.3626$, Student's *t* test) (Fig. 4*A*). Interestingly, orexin A levels in the sham-DMNS group were slightly higher than those in control mice (Fig. 6*B*). This may be due to mechanical irritation of the nerve from the stimulating electrode, which was placed beside the median nerve, and accentuated by respiratory movements of the animal.

Median Nerve Block Prevented MNS-PC6-IA and DMNS-Induced Orexin Elevation. To further substantiate the notion that MNS-PC6-IA results from MNS, we examined whether MNS-PC6-IA was prevented by blocking median nerve conduction with lidocaine. Lidocaine (2%, 10 μL) was injected adjacent to the nerve and 2.0 mm proximally from PC6 before commencing MNS-PC6 (Fig. 6*C*). Interestingly, MNS-PC6 failed to induce antinociception in lidocaine-pretreated mice, and this dose of lidocaine did not significantly affect the hot-plate nociceptive response (Fig. 6 *D* and *E*). Similarly, when lidocaine was locally applied on the exposed median nerves in the DMNS group of mice, orexin A levels were not increased after DMNS (Fig. 6*B*). These results indicate that median nerve block prevents MNS-PC6-IA and DMNS-induced orexin elevation, supporting the notion that MNS-PC6-IA can be attributed to MNS.

Systemic Pretreatment with Opioid Antagonists Did Not Affect MNS-PC6-IA. As shown above, MNS-PC6 caused the release of orexins in the vlPAG to induce analgesia through the OX1R–2-AG–CB1R

sequential cascade (36), which is opioid independent (53). We therefore further examined whether analgesia produced by MNS-PC6 is opioid independent. Systemic pretreatment with naloxone (1 mg/kg, i.p.) did not significantly affect MNS-PC6-IA (Fig. 7). To rule out the possibility that this negative result was due to the short duration of naloxone action, we tested a longer-acting opioid receptor antagonist, naltrexone. Similarly, pretreatment with naltrexone (1 mg/kg) failed to significantly affect MNS-PC6-IA (Fig. 7), suggesting that MNS-PC6-IA is opioid independent in mice. This is in agreement with the clinical observation that s.c. MNS can suppress dysmenorrhea in an opioid-independent manner (25).

MNS-PC6 Suppressed Mechanical Allodynia in a Mouse Neuropathic Pain Model. We further substantiated that MNS-PC6-IA is efficacious in a pathological pain model, a mouse model of neuropathic pain induced by chronic constriction nerve injury (CCI), hereafter, "CCI mice." Neuropathy was induced in mice by ligation of the right sciatic nerve (57). Nociceptive responses to von Frey stimulation shown in Fig. 8*B* demonstrated that CCI mice displayed significant mechanical allodynia 7 d after the surgery compared with the non-CCI group, whose right sciatic nerves were surgically exposed but not ligated (Fig. 8 *B* and *C*, control vs. non-CCI). We then applied MNS-PC6, sham-PC6, or non-MNS on day 8. MNS-PC6, but not non-MNS, significantly attenuated mechanical allodynia in the CCI mice (Fig. 8 *B* and *C*, MNS/vehicle vs. control). Nevertheless, MNS-PC6 did not completely restore the mechanical nociceptive threshold of CCI mice to the level of the non-CCI group (MNS/vehicle vs. non-CCI, $P = 0.0011$, Tukey's test). Interestingly, the sham group that received acupuncture needle insertion but no electrical stimulation showed a slight but significant decrease in the allodynic response compared with the control anesthesia-only CCI mice ($P = 0.0097$, Tukey's test). The cause of this effect remains to be elucidated.

Importantly, the antiallodynic effect of MNS-PC6 in neuropathic mice was prevented by either SB334867 (an OX1R antagonist) or AM 251 (a CB1R antagonist) but not by naloxone (an opioid receptor antagonist) (Fig. 8*C*).

Discussion

Here, we found that MNS-PC6 induced antinociception in two pain models in mice and revealed a mechanism for MNS-PC6-IA using pharmacological, genetic, and neurochemical approaches. Specifically, MNS-PC6 activates hypothalamic orexin neurons, releasing orexins that activate postsynaptic OX1Rs in the vlPAG to generate 2-AG, very likely through a PLC–DAGL enzymatic cascade
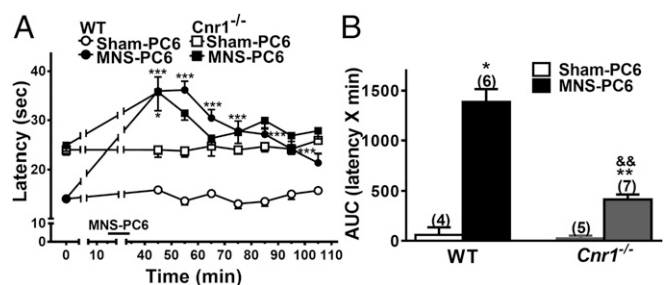

Fig. 5. Effects of MNS-PC6 on the hot-plate test in $Cnr1^{-/-}$ and WT mice. All protocols, statistical analyses, and data presentation, unless stated otherwise, are the same as in Fig. 2. (*A*) The antinociceptive effects of MNS-PC6 in WT and $Cnr1^{-/-}$ mice. Time courses of antinociceptive effects are expressed as the paw-withdrawal latency. ***$P <$ 0.001 vs. the sham group (two-way ANOVA with repeat measures over time/Bonferroni's post hoc test). (*B*) MNS-PC6-IA as indicated by AUCs in WT and $Cnr1^{-/-}$ mice. *$P <$ 0.05/3 vs. the sham group; &&$P <$ 0.01/3 vs. the MNS/WT group (Kruskal–Wallis test/Mann–Whitney *U* post hoc test with the Bonferroni correction). The numbers in parentheses over the bars in *B* indicate the number of mice used in each group.
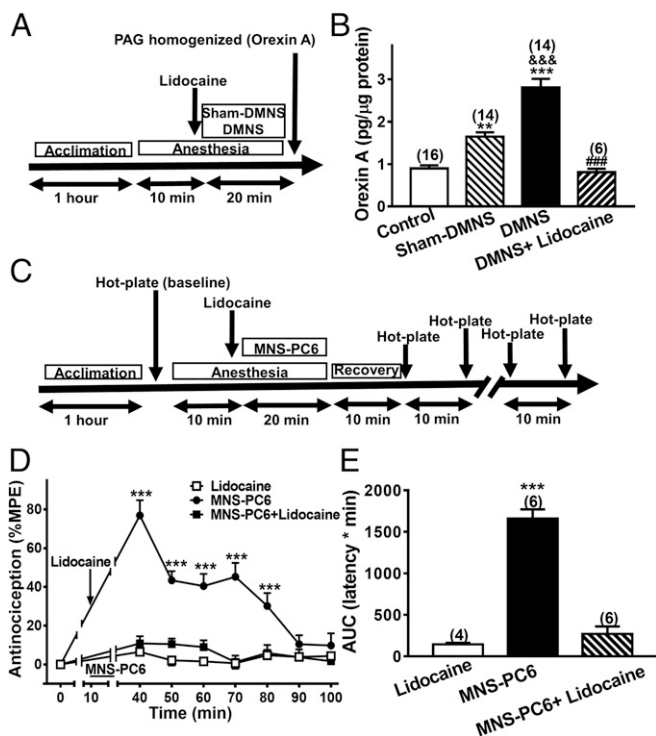
www.manaraa.com

Fig. 6. MNS-PC6 is equivalent to DMNS. (*A*) Timeline for procedures (drug administration, anesthesia, and blood and brain tissue sampling) before and after DMNS on the surgically exposed median nerve. After 1 h of acclimation, mice were anesthetized under 2% isoflurane. Their median nerves were surgically exposed, and they were given DMNS for 20 min. DMNS was performed via electrical stimulation (2 Hz, 1 mA, 0.15 ms) by placing the stimulating electrode next to the surgically exposed right median nerve. The sham-DMNS group received the same procedure as the DMNS group, but electrical stimulation was omitted. The control group received anesthesia only. In the DMNS+lidocaine group, a drop of lidocaine solution (2%) was applied directly onto the median nerve before commencing DMNS. vlPAG homogenates were prepared immediately after DMNS termination for orexin A measurement. (*B*) Orexin A levels in vlPAG homogenates prepared from mice in the DMNS, sham-DMNS, DMNS+lidocaine, and control groups. Immediately after DMNS termination, the vlPAG in each mouse was micropunched bilaterally and homogenized. The orexin A level in the vlPAG homogenate was measured with EIA. $**P <$ 0.01, $***P < 0.001$ vs. control; $^{\&\&\&}P < 0.001$ vs. sham-DMNS; $^{\#\#\#}P < 0.001$ vs. DMNS (one-way ANOVA/Tukey's post hoc test). (*C*) Timeline for procedures, the median nerve block, and the hot-plate tests before and after MNS-PC6. Briefly, the procedure was as shown in Fig. 1, except that lidocaine solution (2%, 10 µL) was injected 2.0 mm proximal to the PC6 acupoint before commencing MNS-PC6. (*D*) The effect of median nerve block by lidocaine injection before MNS-PC6 on MNS-PC6-IA. Time courses of antinociceptive effects are expressed as the percentage of MPE (%MPE). The arrow indicates lidocaine injection; the horizontal bar indicates MNS-PC6. $***P < 0.001$ vs. MNS-PC6+lidocaine (two-way ANOVA with repeated measures over time/Bonferroni's post hoc test) (*E*) Antinociceptive effects, expressed as the AUC in the MNS-PC6 groups without (MNS-PC6) or with median nerve block by lidocaine (MNS-PC6+lidocaine) and in the group treated with lidocaine only. Comparison groups are as in *D*; $***P < 0.001$ vs. MNS-PC6+lidocaine (Dunnett's multiple comparisons test; also see *SI Appendix*, Table S2). The numbers in parentheses over the bars in *B* and *E* indicate the number of mice used in each group.

(36). In turn, 2-AG retrogradely inhibits GABA release via presynaptic CB1Rs in the vlPAG, leading to analgesia through disinhibition of vlPAG outputs (Fig. 9). This MNS-PC6-IA effect is opioid independent and is initiated through acupoint stimulation on the medial nerve dermatome but not by nonspecific electrical stimulation.

MNS-PC6-IA Is Mediated by the Disinhibition Mechanism via the OX1R–PLC–DAGL–2-AG–CB1R Cascade in the vlPAG. It is noteworthy that MNS-PC6-IA was reduced to a similar extent by either

Chen et al.

i.p. or i.pag. injection of SB 334867 or AM251 or by i.pag. injection of THL at doses completely antagonizing an MNS-PC6-IA–comparable antinociceptive effect induced by i.pag. injection of exogenous orexin A (Fig. 2 *C* and *D*) (53). This suggests that the effects of MNS-PC6-IA and exogenous orexin A-induced antinociception share a common mechanism involving OX1Rs, 2-AG, and CB1Rs in the vlPAG. This mechanism is very likely to be the disinhibition mechanism induced by orexin via the OX1R–PLC–DAGL–2-AG–CB1R sequential signaling in the vlPAG, as demonstrated in our previous electrophysiological study (36).

Immunofluorescence, EIA, and microdialysis assessments provide direct evidence supporting the premise that MNS-PC6, but not stimulation of a nonmedian nerve-innervated location, activates LH orexin neurons (Fig. 3), increases orexin A levels (Fig. 4*A*), and decreases GABA levels in the vlPAG (Fig. 4*B*). Therefore, our results demonstrate that MNS-PC6 can induce analgesia via releasing orexins from the LH to inhibit GABA release in the vlPAG through an OX1R–DAGL–2-AG–CB1R cascade. We further demonstrated that the MNS-PC6-IA effect is not due to a nonspecific electrical stimulation, since electrical stimulation at the lateral deltoid muscle, a nonmedian nerve-innervated location, was unable to induce analgesia (Figs. 2 *A* and *B* and 8 *B* and *C*), activate LH orexin neurons (Fig. 3), increase orexin levels (Fig. 4*A*), or decrease GABA levels in the vlPAG (Fig. 4*B*).

MNS-PC6 and EA-PC6. In the present study, the Neiguan (PC6) acupoint was chosen as a standardized location to insert the acupuncture needle for MNS. The location of PC6 was based on the anatomical description in the WHO guidelines for human acupoints (58). Therefore, this procedure (MNS-PC6) is equivalent to EA-PC6 in Chinese medicinal practice. Several reports have validated the association between EA-PC6 and MNS. First, PC6 overlies a dermatome of the median nerve (49). Second, the anatomical location of PC6 is highly similar to the stimulation site described in several peripheral neuromodulation studies in humans in which percutaneous and s.c. electrical stimulations at the median nerve have been conducted (26, 27, 49, 59). Third, the median nerve was reported to be crucial for EA-PC6 (60). Fourth, the effects induced by EA-PC6 in Chinese medicine practice (59) are similar to the effects induced by peripheral neuromodulation, especially by MNS (17).

In this animal study, we provide direct evidence that MNS-PC6, the EA-PC6 procedure used in Chinese medicine, is a type
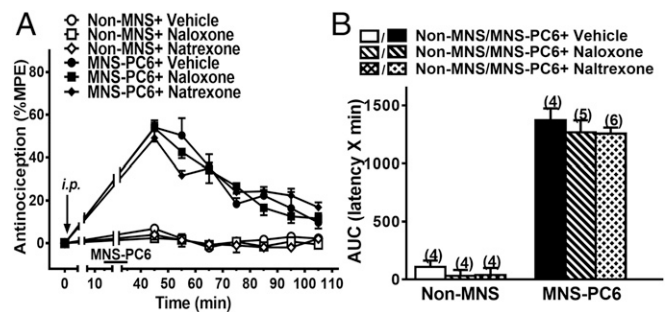

Fig. 7. The analgesic effect of MNS-PC6 was not reversed by pretreatment with naloxone or naltrexone. All protocols, statistical analyses, and data presentation, unless stated otherwise, are the same as in Fig. 2. Antinociceptive effects in the MNS-PC6, non-MNS, and vehicle groups of mice without or with i.p. pretreatment with naloxone (1 mg/kg) or naltrexone (1 mg/kg) are shown as percent MPE (*A*) (two-way ANOVA with repeat measures over time/Bonferroni's post hoc test) and as AUC (*B*) (Kruskal–Wallis test/Mann–Whitney *U* post hoc test with the Bonferroni correction with *n* independent hypotheses; also see *SI Appendix*, Table S2). The numbers in parentheses over the bars in *B* indicate the number of mice used in each group.
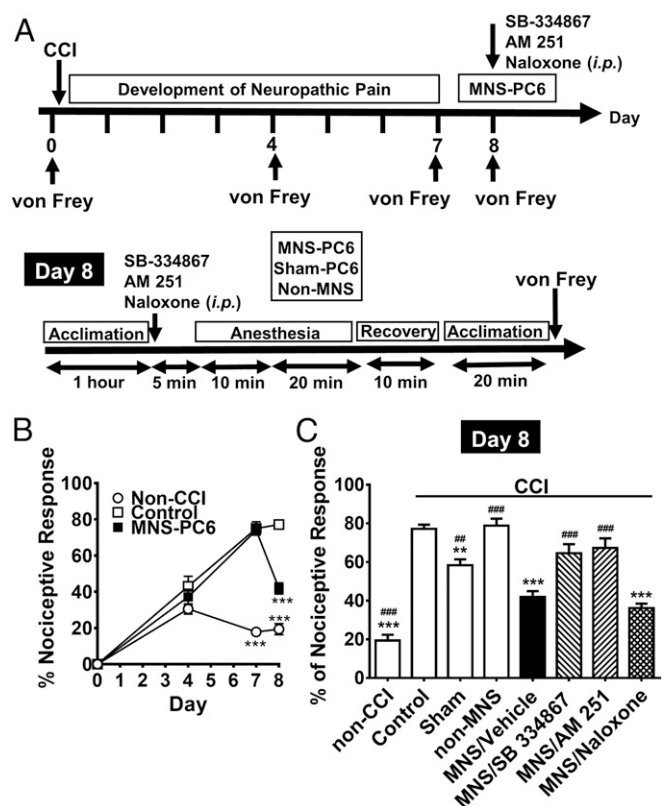
NEUROSCIENCE

Fig. 8. MNS-PC6 attenuated CCI-induced mechanical allodynia via OX1Rs and CB1Rs but not via opioid receptors. (*A*) Mice received CCI surgery on day 0 and developed neuropathy, evidenced by mechanical allodynia of the injured hind paw, by day 7. MNS-PC6, sham-PC6, and non-MNS carried out as in Fig. 1 were applied to CCI mice on day 8. Mechanical sensitivity of the hind paw to a von Frey filament (0.16 g) was measured. (*B*) Mechanical allodynia, measured by the percentage of positive nociceptive responses (withdrawal, flinching, or licking) during 10 trials of von Frey filament stimulation, developed in CCI mice. Note that mechanical allodynia developed gradually and peaked 7 d after CCI. On day 8, MNS-PC6 significantly reduced mechanical allodynia in CCI mice compared with the control group (CCI mice receiving anesthesia only). (*C*) Allodynic responses in mice not receiving CCI (non-CCI) or in CCI-mice receiving anesthesia only (control), sham-PC6 (sham), non-MNS, and MNS-PC6 procedures, as well as in the MNS-PC6 group i.p. pretreated with an OX1R antagonist (SB 334867, 15 mg/kg, i.p.), a CB1R antagonist (AM251, 1.1 mg/kg, i.p.), an opioid receptor antagonist (naloxone, 1 mg/kg, i.p.) or vehicle. Note that CCI-induced mechanical allodynia was significantly reduced by MNS-PC6 but not by non-MNS. The MNS-PC6–induced antiallodynic effect was prevented by SB 334867 or AM251 but not by naloxone. **$P < 0.01$, ***$P < 0.001$ vs. control; ##$P < 0.01$, ###$P < 0.001$ vs. MNS-PC6/vehicle (one-way ANOVA with Tukey's post hoc test).

of MNS. First, DMNS, like MNS-PC6 (Fig. 4*A*), also increased orexin A levels in the vlPAG, and this effect was blocked by applying lidocaine to the median nerve (Fig. 6*B*). Second, the MNS-PC6–induced analgesia was prevented when the median nerve was proximally blocked by lidocaine (Fig. 6 *D* and *E*).

The MNS-PC6 procedure employed here is similar to the clinical procedure of percutaneous electrical nerve stimulation targeting the median nerve, which was recently approved by the FDA for pain relief (6, 7). The finding that MNS-PC6 significantly increased the pain threshold for noxious heat in mice is consistent with the clinical reports that MNS increased the thresholds for somatosensation (61) and pain (62) in healthy volunteers.

The Longhurst group (47, 48) reported that EA at the PC5–PC6 acupoints in rats reduced GABA levels in the vlPAG in an AM251-sensitive manner. Using the same electrical stimulation parameters, we found a CB1R-dependent GABA reduction in

vlPAG microdialysates in mice receiving MNS-PC6. Importantly, this MNS-PC6–induced GABA reduction was prevented by blocking OX1Rs, suggesting it requires orexins released during MNS-PC6. In this study, not only MNS-PC6 but also DMNS induced orexin release in mice. Interestingly, MNS was recently reported to be able to induce orexin release from the LH and increase arousal in a rat coma model (63, 64). It is suggested that EA-PC6 and MNS share the same effect, releasing orexins into the vlPAG.

MNS-PC6-IA Is Opioid Independent. MNS-PC6-IA is opioid independent, because it was not significantly affected by the opioid antagonists naloxone or naltrexone (Figs. 7 and 8*C*). This is consistent with the opioid-independent nature of orexin-induced antinociception reported previously (65–67) and also with a clinical report that MNS-induced analgesia was not reversed by naloxone in patients (25). Furthermore, based on clinical observations, it is unlikely that MNS-PC6-IA would be opioid dependent, as there have been no reports of analgesic tolerance in patients receiving MNS with implanted stimulators after several years of use (19, 23, 24).

Given that MNS-PC6 as employed here is a procedure similar to EA-PC6, the finding that MNS-PC6-IA is opioid independent is noteworthy. It conflicts with the endogenous opioid theory that has long been suggested for acupuncture-induced analgesia (68). The discrepancy may be due to the different locations of the acupoints and hence the different peripheral nerves that were stimulated. From our literature search, most previous studies on acupuncture analgesia were performed via stimulating the ST36 (Zusanli) acupoint, which is near the tibial nerve (68–70). Therefore, whether acupuncture analgesia is mediated by endogenous opioids may depend on the location of the acupoints and thus the adjacent peripheral nerves that are stimulated. It remains to be elucidated whether the orexin- and endocannabinoid-mediated analgesia mechanism found in this study also contributes to the analgesic effects elicited when other acupoints or peripheral nerves are stimulated.

Study Limitations. There are several limitations in this study. First, in this animal study, MNS was performed in mice under anesthesia. In contrast, patients in clinical settings receive peripheral neuromodulation or acupuncture without anesthesia. Second, how electrical stimulation at acupoints and the median nerve peripherally can lead to central activation of the LH orexin neurons remains to be clarified. Third, whether this nonopioid MNS-induced analgesic mechanism is effective in other pain models, such as pain associated with cancer, arthritis, or chronic inflammation, is unknown and warrants future studies.

Conclusions and Perspectives. Peripheral nerve stimulation, including MNS, has been applied for the relief of intractable chronic pain for over 50 y, and acupuncture analgesia has been used in Chinese medicine for thousands of years. However, their mechanism(s) remain unclear, although an endogenous opioid theory has been proposed. Here, we revealed a nonopioid analgesic mechanism for MNS via the PC6 acupoint, which is mediated by OX1R-initiated endocannabinoid retrograde disinhibition in the vlPAG. It is induced by median nerve stimulation, especially at the PC6 acupoint. It has long been argued that the analgesic effect of acupuncture is merely a placebo effect in humans (71). Here, through animal experiments, we substantiated that MNS-PC6, the procedure equivalent to EA-PC6, can induce analgesia. EA-PC6 is a type of MNS, but EA-PC6 does not stimulate only the median nerve, as other neural and motor components underlying the PC6 acupoint may also contribute to the effect of EA-PC6. Adequate treatment of pain, especially neuropathic pain and cancer pain, remains an unmet medical need due to the significant adverse effects and limitations
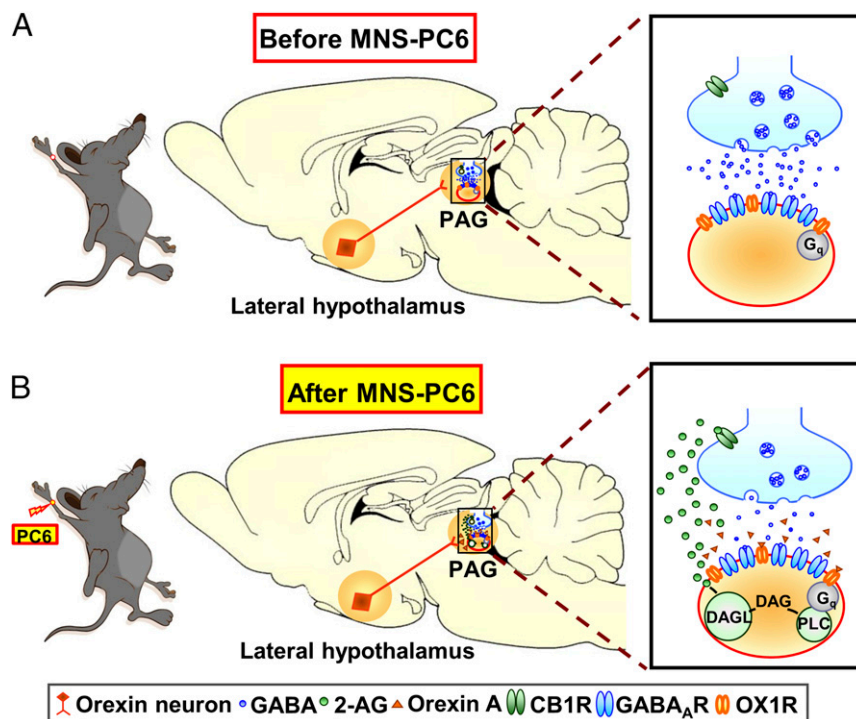
www.manaraa.com

Fig. 9. A mechanism for MNS-PC6-induced analgesia. This schema describes events occurring in the LH and the PAG before (*A*) and after (*B*) MNS-PC6–induced analgesia. (*Left*) The locations of the PC6 acupoint and non-MNS in a mouse are schematically depicted on the cartoon mouse figure. The cartoons (*Right*) are enlarged views of the synaptic events occurring in the PAG (*Center*). During MNS-PC6, the LH orexin neurons (•) projecting to the PAG are activated. The released orexins (▲) then activate postsynaptic OX1Rs (▯) in the PAG. Activation of the OX1R, a Gq-protein–coupled receptor, activates PLC to generate diacylglycerol (DAG), which can be converted into 2-AG (●), an endocannabinoid, by DAGL. 2-AG then travels retrogradely across the synapse to inhibit GABA (○) release by activating presynaptic CB1Rs (▯). Inhibition of GABAergic synaptic neurotransmission in the vlPAG activates the descending pain inhibitory pathway, leading to analgesia. This disinhibition mechanism in the vlPAG, mediated by the OX1R–PLC–DAGL–2-AG–CB1R cascade, primarily mediates MNS-PC6-IA (▭).

of current analgesics as well as the potential risk of opioid misuse (72). The present study provides solid justification for the investigation of MNS as an alternate pain-management strategy, especially in patients with opioid tolerance, because the unique supraspinal mechanism of MNS-PC6-IA involves an opioid-independent and orexin-initiated endocannabinoid pathway. It remains to be elucidated if this mechanism extends to other MNS/acupuncture regimens related to orexin functions, such as sleeping, eating, addiction, and depression (73), or to cannabinoid functions, such as the therapeutic benefit of EA-PC6 on nausea and vomiting (74–76).

Materials and Methods

Please see *SI Appendix, SI Materials and Methods* for the protocols and methods of i.pag. microinjection, double immunolabeling of c-Fos and orexin A, EIA of orexin A in the vlPAG homogenate, and drugs and for the details of animals used.

Animals. Male adult C57BL/6 mice aged 8–10 wk were used for all experiments. *Cnr1*$^{-/-}$ mice were generated as reported previously (56) and were bred in the National Health Research Institutes (NHRI), Zhunan, Miaoli, Taiwan. All experiments adhered to the guidelines approved by the Institutional Animal Care and Use Committees in the College of Medicine, National Taiwan University and the NHRI.

MNS-PC6. On the experimental day, mice were moved in their home cages to a behavioral room and were acclimated there for 1 h before testing. Mice were randomly divided into four groups for studying the effects of MNS-PC6: the MNS-PC6 group, the sham-operated group, a non-MNS group, and a control group. Mice were anesthetized by 2% isoflurane. The MNS-PC6 group received low-frequency electrical stimulation (2 Hz, 2 mA, 0.15 ms) for 20 min by an electrical stimulator (Trio 300; ITO Co.) through acupuncture needles inserted bilaterally at the PC6 (Neiguan) acupoint. The proportional locations

of the PC6 acupoint and the non-MNS region in mouse (*SI Appendix,* Fig. S1) were determined following the anatomical description in the WHO guidelines for human acupoints (58). The non-MN region selected was located in the middle of the lateral deltoid muscle, a nonmedian nerve-innervated location. In humans, the PC6 acupoint is located on the anterior aspect of the forearm, between the palmaris longus and flexor carpi radialis tendons, proximal to the wrist crease, one-sixth of the distance between the wrist and cubital creases. Thus, in mice, PC6 is located at one-sixth of the anterior forelimb length above the rasceta between the ulna and the radius. Acupuncture needles (32-gauge; Yu Kuang) were inserted perpendicularly to a depth of 1–3 mm at the PC6 or non-MNS location bilaterally. Successful stimulation of PC6 through the needle was confirmed by the presence of paw twitches during MNS-PC6 stimulation (47, 48). After MNS-PC6, mice were allowed to recover completely from anesthesia for 10 min before being subjected to the hot-plate test (Fig. 1). The sham group received only needle insertion bilaterally at the PC6 acupoint with no electrical stimulation. The non-MNS group received the same electrical stimulation (2 Hz, 2 mA, 0.15 ms) through acupuncture needles inserted bilaterally in the middle of the lateral deltoid muscle. The control group received no treatment except anesthesia and vehicle injection, if stated. The sham group, non-MNS group, and control group underwent the same anesthesia and recovery procedures. To examine the effect of median nerve block on MNS-PC6-IA, anesthetized mice received bilateral injections of lidocaine (2%, 10 μL) 2.0 mm proximal to the PC6-acupoint before the electrical stimulation procedure.

DMNS. To study DMNS effects, mice were divided into DMNS, sham-DMNS, and control groups. In the DMNS group, the right median nerve was surgically exposed and directly stimulated via a bipolar platinum electrode at the same parameters as MNS (2 Hz, 20 ms) but with a reduced current (1.0 mA). In the sham-DMNS group, the stimulating electrode was placed beside the median nerve without activating the power. The control group received anesthesia only. After DMNS, mice were killed, and the vlPAG tissues were collected for EIA of orexin A. For the median nerve block experiment, a

Chen et al.

drop of 2% lidocaine solution was applied onto the exposed median nerve before DMNS.

The Hot-Plate Test. The paw-withdrawal latency to thermal stimulation on a hot plate of 49 °C in the mouse was determined as reported previously (36, 77), with modifications. The withdrawal cutoff time was 60 s to avoid heat-induced paw damage. For MNS-PC6-IA experiments, the hot-plate test was conducted in mice before any treatment, 10 min after the termination of MNS (at that time mice have completely recovered from anesthesia), and every 10 min thereafter for 60 min in total (Fig. 1). For orexin A (i.pag.)-induced antinociception experiments, the hot-plate test was conducted before and 5 min after orexin A microinjection and then was conducted every 10 min for 60 min. The antinociceptive effect in each mouse at each time point was calculated as the percentage of maximal possible effect (MPE) by the equation: %MPE = 100 × (Latency$_{after\ treatment}$ − Latency$_{before\ treatment}$)/ (60 s − Latency$_{before\ treatment}$). The AUC of withdrawal latencies during the 60-min recording period was calculated as the total antinociceptive effect in each mouse.

CCI Surgery in Mice. The CCI surgery in mice was conducted as reported previously (78). Briefly, under anesthesia with sodium pentobarbital (80 mg/kg, i.p.), the right sciatic nerve was exposed and loosely ligated with a 4.0 silk suture. The incision was then closed, and mice were returned to their home cages. Neuropathic pain was well established 7 d after the CCI surgery, as evidenced by mechanical allodynia in the hind paw of the injured side (Fig. 8B) (57). Eight days after CCI, the mechanical allodynic response was evaluated by the percentage of positive responses (withdrawal, flinching, or licking) to a total of 10 repetitive stimulations with a von Frey filament exerting 0.16 g of force onto the plantar surface of the paw on the injured side (79).

Measurement of GABA Levels in vlPAG Microdialysates.

IntravlPAG microdialysis cannulation. While under sodium pentobarbital anesthesia (i.p. 80 mg/kg), mice were implanted with a microdialysis guide cannula aimed at the vlPAG following the stereotaxic coordinates of the mouse described above (80). After cannulation mice were allowed to recover for a minimum of 7 d before microdialysis.

In vivo microdialysis. Microdialysis was performed in the vlPAG of anesthetized mice with a method modified from a previous report. In brief, on the day of the microdialysis experiment, each mouse was lightly anesthetized by 2% isofluorane, and a microdialysis probe [MAB 10.8.1, 6 kDa cutoff, 1 mm poly (ethyl sulfone) membrane; Microbiotech/se AB] was inserted through the implanted guide cannula. The probes were perfused (1 μL/min) with an artificial CSF solution consisting of (in mM) 149 NaCl, 2.8 KCl, 1.2 CaCl$_2$, 1.2 MgCl$_2$, 0.25 ascorbic acid, and 5.4 D-glucose. Two hours after probe implantation, dialysate samples were collected on ice from 75 to 55, 55–35, and 20–0 min before, during, and every 20 min after MNS-PC6 or non-MNS treatment for 1 h in each mouse. After the experiment, the brain was removed and cryoprotected, sectioned at 50 μm on a cryostat, and stained with cresyl violet (Nissl stain) to confirm the probe location (*SI Appendix*, Fig. S3).

GABA measurement. GABA levels in the microdialysate of the mouse were measured by HPLC as reported previously (81–83), with modifications. In brief, for a precolumn derivation, the microdialysate (20 μL) was mixed with 10 μL o-phthaldialdehyde (OPA) solution (10 mg of OPA, 0.5 mL of methanol, 4 mL of 0.4 M borate buffer, and 10 μL of β-mercaptaoethanol) for 45 s at room temperature. The GABA level in the mixed sample was then immediately measured by HPLC. The mobile phase solution for isocratic elution of GABA, consisting of 60% 0.1 M acetate buffer (pH 5), 40% methanol, and 2 mM KCl, was run through a C18, 3-μm HPLC analytical column (Grace) and was pumped using an S 1130 HPLC pump system (Sykam GmbH) at a flow rate of 0.2 mL/min. The GABA level was detected by a DECADE II Electrochemical Detector (Antec Scientific). The peak identity was confirmed by concurrent samples with standard GABA solutions ranging from 10 to 100 pM (*SI Appendix*, Fig. S4).

Statistical Analysis. The SPSS software package for Windows (IBM Analytics) was used for statistical analyses. Data are expressed as the mean ± SEM; n indicates the number of mice tested. Before the experiments were conducted, the sample size for each group was estimated using the SD values from a pilot study in mice and our previous studies on orexin-induced antinociceptive effects in rats (36) with an expected power of 80%. We checked all data with either the ROUT or Grubbs method, and no outliers were found; Q = 1% by ROUT and alpha = 0.05 by the Grubbs method. Furthermore, the Shapiro–Wilk test was employed to verify that all data are normally distributed. Therefore, for the time-course figures depicting antinociceptive effects, differences among groups were analyzed using the parametric two-way ANOVA with repeated measures over time. Differences between two groups at each time point were analyzed by Bonferroni's post hoc test. P values of <0.05 were considered statistically significant. For the comparisons of the AUCs of antinociceptive effects among groups, the nonparametric Kruskal–Wallis test was used, since the variances in each group were not equal. Differences between two compared groups were analyzed post hoc by the two-sided Mann–Whitney U test with the Bonferroni correction. The significance level was set at 0.05/n, where n is the number of independent hypotheses tested. Most of the data of c-Fos–expressing LH orexin neuronal numbers, vlPAG orexin A levels, and plasma corticosterone levels were normally distributed with equal variance. Therefore, one-way ANOVA followed by Tukey's post hoc test was used for these experimental data.

1. Abbasi J (2018) Robert Kerns, PhD: Researching nondrug approaches to pain management. *JAMA* 319:1535–1537.
2. Wall PD, Sweet WH (1967) Temporary abolition of pain in man. *Science* 155:108–109.
3. Melzack R, Wall PD (1965) Pain mechanisms: A new theory. *Science* 150:971–979.
4. Goroszeniuk T, Pang D (2014) Peripheral neuromodulation: A review. *Curr Pain Headache Rep* 18:412.
5. Slavin KV (2011) *Peripheral Nerve Stimulation* (S. Karger AG, Basel).
6. Reddy CG, et al. (2017) Novel technique for trialing peripheral nerve stimulation: Ultrasonography-guided StimuCath trial. *Neurosurg Focus* 42:E5.
7. Food and Drug Administration (2016) StimQ Peripheral Nerve Stimulator (PNS) System: 510(k) Premarket Notification. Available at https://www.accessdata.fda.gov/scripts/cdrh/cfdocs/cfpmn/pmn.cfm?ID=K152178. Accessed January 29, 2018.
8. Mendell LM (2014) Constructing and deconstructing the gate theory of pain. *Pain* 155:210–216.
9. Vera-Portocarrero L (2014) Mechanism of spinal cord and peripheral nerve stimulation: More than the gate control theory. Replace, repair, restore, relieve–Bridging clinical and engineering solutions in neurorehabilitation. *Proceedings of the Second International Conference on NeuroRehabilitation (ICNR2014), Aalborg, 24-26 June, 2014*, eds Jensen W, Andersen OK, Akay M (Springer International Publishing, Cham, Switzerland), pp 135–136.
10. Bartsch T, Goadsby PJ (2011) Central mechanisms of peripheral nerve stimulation in headache disorders. *Prog Neurol Surg* 24:16–26.
11. Swett JE, Law JD (1983) Analgesia with peripheral-nerve stimulation–Absence of a peripheral mechanism. *Pain* 15:55–70.
12. Campbell JN, Taub A (1973) Local analgesia from percutaneous electrical stimulation. A peripheral mechanism. *Arch Neurol* 28:347–350.
13. Kalra A, Urban MO, Sluka KA (2001) Blockade of opioid receptors in rostral ventral medulla prevents antihyperalgesia produced by transcutaneous electrical nerve stimulation (TENS). *J Pharmacol Exp Ther* 298:257–263.
14. Men DS, Matsui Y (1994) Activation of descending noradrenergic system by peripheral nerve stimulation. *Brain Res Bull* 34:177–182.
15. Men DS, Matsui Y (1994) Peripheral nerve stimulation increases serotonin and dopamine metabolites in rat spinal cord. *Brain Res Bull* 33:625–632.
16. Shetter AG, Racz GB, Lewis R, Heavner JE (1997) Peripheral nerve stimulation. *Neurosurgical Management of Pain*, eds North RB, Levy RM (Springer, New York), pp 261–270.
17. Mirone G, Natale M, Rotondo M (2009) Peripheral median nerve stimulation for the treatment of iatrogenic complex regional pain syndrome (CRPS) type II after carpal tunnel surgery. *J Clin Neurosci* 16:825–827.
18. Jeon IC, Kim MS, Kim SH (2009) Median nerve stimulation in a patient with complex regional pain syndrome type II. *J Korean Neurosurg Soc* 46:273–276.
19. Van Calenbergh F, et al. (2009) Long term clinical outcome of peripheral nerve stimulation in patients with chronic peripheral neuropathic pain. *Surg Neurol* 72:330–335, discussion 335.
20. Mobbs RJ, Nair S, Blum P (2007) Peripheral nerve stimulation for the treatment of chronic pain. *J Clin Neurosci* 14:216–221; discussion 222–213.
21. Strege DW, Cooney WP, Wood MB, Johnson SJ, Metcalf BJ (1994) Chronic peripheral nerve pain treated with direct electrical nerve stimulation. *J Hand Surg Am* 19:931–939.

22. Campbell JN, Long DM (1976) Peripheral nerve stimulation in the treatment of intractable pain. *J Neurosurg* 45:692–699.

23. Eisenberg E, Waisbrod H, Gerbershagen HU (2004) Long-term peripheral nerve stimulation for painful nerve injuries. *Clin J Pain* 20:143–146.

24. Nashold BS, Jr, Goldner JL, Mullen JB, Bright DS (1982) Long-term pain control by direct peripheral-nerve stimulation. *J Bone Joint Surg Am* 64:1–10.

25. Walker JB, Katz RL (1981) Non-opioid pathways suppress pain in humans. *Pain* 11:347–354.

26. Walker JB, Katz RL (1981) Peripheral nerve stimulation in the management of dysmenorrhea. *Pain* 11:355–361.

27. Lee M, Kiernan MC, Macefield VG, Lee BB, Lin CS (2015) Short-term peripheral nerve stimulation ameliorates axonal dysfunction after spinal cord injury. *J Neurophysiol* 113:3209–3218.

28. Chung JM, Lee KH, Hori Y, Endo K, Willis WD (1984) Factors influencing peripheral nerve stimulation produced inhibition of primate spinothalamic tract cells. *Pain* 19:277–293.

29. Basbaum AI, Fields HL (1978) Endogenous pain control mechanisms: Review and hypothesis. *Ann Neurol* 4:451–462.

30. Porreca F, Ossipov MH, Gebhart GF (2002) Chronic pain and medullary descending facilitation. *Trends Neurosci* 25:319–325.

31. Tracey I, Mantyh PW (2007) The cerebral signature for pain perception and its modulation. *Neuron* 55:377–391.

32. Gerhart KD, Yezierski RP, Wilcox TK, Willis WD (1984) Inhibition of primate spinothalamic tract neurons by stimulation in periaqueductal gray or adjacent midbrain reticular formation. *J Neurophysiol* 51:450–466.

33. Carstens E (1988) Inhibition of rat spinothalamic tract neuronal responses to noxious skin heating by stimulation in midbrain periaqueductal gray or lateral reticular formation. *Pain* 33:215–224.

34. Young RF, Chambi VI (1987) Pain relief by electrical stimulation of the periaqueductal and periventricular gray matter. Evidence for a non-opioid mechanism. *J Neurosurg* 66:364–371.

35. Jacquet YF, Lajtha A (1973) Morphine action at central nervous system sites in rat: Analgesia or hyperalgesia depending on site and dose. *Science* 182:490–492.

36. Ho YC, et al. (2011) Activation of orexin 1 receptors in the periaqueductal gray of male rats leads to antinociception via retrograde endocannabinoid (2-arachidonoylglycerol)-induced disinhibition. *J Neurosci* 31:14600–14610.

37. Martin WJ, Patrick SL, Coffin PO, Tsou K, Walker JM (1995) An examination of the central sites of action of cannabinoid-induced antinociception in the rat. *Life Sci* 56:2103–2109.

38. de Lecea L, et al. (1998) The hypocretins: Hypothalamus-specific peptides with neuroexcitatory activity. *Proc Natl Acad Sci USA* 95:322–327.

39. Sakurai T, et al. (1998) Orexins and orexin receptors: A family of hypothalamic neuropeptides and G protein-coupled receptors that regulate feeding behavior. *Cell* 92:573–585.

40. Peyron C, et al. (1998) Neurons containing hypocretin (orexin) project to multiple neuronal systems. *J Neurosci* 18:9996–10015.

41. van den Pol AN (1999) Hypothalamic hypocretin (orexin): Robust innervation of the spinal cord. *J Neurosci* 19:3171–3182.

42. Date Y, et al. (1999) Orexins, orexigenic hypothalamic peptides, interact with autonomic, neuroendocrine and neuroregulatory systems. *Proc Natl Acad Sci USA* 96:748–753.

43. Sakurai T (2006) Roles of orexins and orexin receptors in central regulation of feeding behavior and energy homeostasis. *CNS Neurol Disord Drug Targets* 5:313–325.

44. Behbehani MM, Jiang MR, Chandler SD, Ennis M (1990) The effect of GABA and its antagonists on midbrain periaqueductal gray neurons in the rat. *Pain* 40:195–204.

45. Cristino L, et al. (2016) Orexin-A and endocannabinoid activation of the descending antinociceptive pathway underlies altered pain perception in leptin signaling deficiency. *Neuropsychopharmacology* 41:508–520.

46. Cristino L, Imperatore R, Palomba L, Di Marzo V (2017) The endocannabinoid system in leptin-driven changes of orexinergic signaling under physiological and pathological conditions. *Endocannabinoids and Lipid Mediators in Brain Functions*, ed Melis M (Springer International Publishing, Cham, Switzerland), pp 1–26.

47. Fu LW, Longhurst JC (2009) Electroacupuncture modulates vlPAG release of GABA through presynaptic cannabinoid CB1 receptors. *J Appl Physiol (1985)* 106:1800–1809.

48. Tjen-A-Looi SC, Li P, Longhurst JC (2009) Processing cardiovascular information in the vlPAG during electroacupuncture in rats: Roles of endocannabinoids and GABA. *J Appl Physiol (1985)* 106:1793–1799.

49. Wang K, Liu J (1989) Needling sensation receptor of an acupoint supplied by the median nerve–Studies of their electro-physiological characteristics. *Am J Chin Med* 17:145–155.

50. Ho CY, et al. (2014) Clinical effectiveness of acupuncture for carpal tunnel syndrome. *Am J Chin Med* 42:303–314.

51. Guo ZL, Longhurst JC (2010) Activation of reciprocal pathways between arcuate nucleus and ventrolateral periaqueductal gray during electroacupuncture: Involvement of VGLUT3. *Brain Res* 1360:77–88.

52. Wang KM, Yao SM, Xian YL, Hou ZL (1985) A study on the receptive field of acupoints and the relationship between characteristics of needling sensation and groups of afferent fibres. *Sci Sin [B]* 28:963–971.

53. Lee HJ, et al. (2016) Stress induces analgesia via orexin 1 receptor-initiated endocannabinoid/CB1 signaling in the mouse periaqueductal gray. *Neuropharmacology* 105:577–586.

54. Hadváry P, Sidler W, Meister W, Vetter W, Wolfer H (1991) The lipase inhibitor tetrahydrolipstatin binds covalently to the putative active site serine of pancreatic lipase. *J Biol Chem* 266:2021–2027.

55. Sagar SM, Sharp FR, Curran T (1988) Expression of c-fos protein in brain: Metabolic mapping at the cellular level. *Science* 240:1328–1331.

56. Zimmer A, Zimmer AM, Hohmann AG, Herkenham M, Bonner TI (1999) Increased mortality, hypoactivity, and hypoalgesia in cannabinoid CB1 receptor knockout mice. *Proc Natl Acad Sci USA* 96:5780–5785.

57. Osikowicz M, Mika J, Makuch W, Przewlocka B (2008) Glutamate receptor ligands attenuate allodynia and hyperalgesia and potentiate morphine effects in a mouse model of neuropathic pain. *Pain* 139:117–126.

58. World Health Organization (2008) *WHO Standard Acupuncture Point Locations in the Western Pacific Region* (WHO Western Pacific Region, Manila, Philippines).

59. Xia DD, et al. (2010) [Morphologic characteristics and clinical significance of Neiguan (PC 6)]. *Zhongguo Zhen Jiu* 30:1003–1006. Chinese.

60. Zhou F, Huang D, YingXia (2010) Neuroanatomic basis of acupuncture points. *Acupuncture Therapy for Neurological Diseases*, eds Xia Y, Cao X, Wu G, Cheng J (Springer, Berlin), pp 32–80.

61. Dean J, Bowsher D, Johnson MI (2006) The effects of unilateral transcutaneous electrical nerve stimulation of the median nerve on bilateral somatosensory thresholds. *Clin Physiol Funct Imaging* 26:314–318.

62. Hoshiyama M, Kakigi R (2000) After-effect of transcutaneous electrical nerve stimulation (TENS) on pain-related evoked potentials and magnetic fields in normal subjects. *Clin Neurophysiol* 111:717–724.

63. Zhong YJ, Feng Z, Wang L, Wei TQ (2015) Wake-promoting actions of median nerve stimulation in TBI-induced coma: An investigation of orexin-A and orexin receptor 1 in the hypothalamic region. *Mol Med Rep* 12:4441–4447.

64. Feng Z, Du Q (2016) Mechanisms responsible for the effect of median nerve electrical stimulation on traumatic brain injury-induced coma: Orexin-A-mediated N-methyl-D-aspartate receptor subunit NR1 upregulation. *Neural Regen Res* 11:951–956.

65. Bingham S, et al. (2001) Orexin-A, an hypothalamic peptide with analgesic properties. *Pain* 92:81–90.

66. Mobarakeh JI, et al. (2005) Enhanced antinociception by intracerebroventricularly and intrathecally-administered orexin A and B (hypocretin-1 and -2) in mice. *Peptides* 26:767–777.

67. Chiou LC, et al. (2010) Orexins/hypocretins: Pain regulation and cellular actions. *Curr Pharm Des* 16:3089–3100.

68. Han Z, et al. (1999) Endomorphin-1 mediates 2 Hz but not 100 Hz electroacupuncture analgesia in the rat. *Neurosci Lett* 274:75–78.

69. Kim JH, Min BI, Na HS, Park DS (2004) Relieving effects of electroacupuncture on mechanical allodynia in neuropathic pain model of inferior caudal trunk injury in rat: Mediation by spinal opioid receptors. *Brain Res* 998:230–236.

70. Wang Y, Zhang Y, Wang W, Cao Y, Han JS (2005) Effects of synchronous or asynchronous electroacupuncture stimulation with low versus high frequency on spinal opioid release and tail flick nociception. *Exp Neurol* 192:156–162.

71. Zheng YC, Yuan TT, Liu T (2014) Is acupuncture a placebo therapy? *Complement Ther Med* 22:724–730.

72. Schneiderhan J, Clauw D, Schwenk TL (2017) Primary care of patients with chronic pain. *JAMA* 317:2367–2368.

73. Tsujino N, Sakurai T (2009) Orexin/hypocretin: A neuropeptide at the interface of sleep, energy homeostasis, and reward system. *Pharmacol Rev* 61:162–176.

74. Dundee JW (1990) Electro-acupuncture and postoperative emesis. *Anaesthesia* 45:789–790.

75. Dundee JW, Ghaly RG, Fitzpatrick KT, Lynch GA, Abram WP (1987) Acupuncture to prevent cisplatin-associated vomiting. *Lancet* 1:1083.

76. Dundee JW, Yang J, McMillan C (1991) Non-invasive stimulation of the P6 (Neiguan) antiemetic acupuncture point in cancer chemotherapy. *J R Soc Med* 84:210–212.

77. Lotfipour S, et al. (2013) Targeted deletion of the mouse α2 nicotinic acetylcholine receptor subunit gene (Chrna2) potentiates nicotine-modulated behaviors. *J Neurosci* 33:7728–7741.

78. Ming-Tatt L, et al. (2013) Anti-hyperalgesic effect of a benzilidine-cyclohexanone analogue on a mouse model of chronic constriction injury-induced neuropathic pain: Participation of the κ-opioid receptor and KATP. *Pharmacol Biochem Behav* 114–115:58–63.

79. Goldman N, et al. (2010) Adenosine A1 receptors mediate local anti-nociceptive effects of acupuncture. *Nat Neurosci* 13:883–888.

80. Franklin KBJ, Paxinos G (1997) *Mouse Brain in Stereotaxic Coordinates* (Academic, San Diego).

81. Qi J, et al. (2012) Oxytocin regulates changes of extracellular glutamate and GABA levels induced by methamphetamine in the mouse brain. *Addict Biol* 17:758–769.

82. Stork O, Ji FY, Obata K (2002) Reduction of extracellular GABA in the mouse amygdala during and following confrontation with a conditioned fear stimulus. *Neurosci Lett* 327:138–142.

83. Caillé S, Alvarez-Jaimes L, Polis I, Stouffer DG, Parsons LH (2007) Specific alterations of extracellular endocannabinoid levels in the nucleus accumbens by ethanol, heroin, and cocaine self-administration. *J Neurosci* 27:3695–3702.

NEUROSCIENCE

Chen et al.

www.manaraa.com